ARTICLE

Multi-Source/Component Spray Coating for Polymer Solar Cells

Li-Min Chen,[†,§] Ziruo Hong,[†,§] Wei Lek Kwan,[†] Cheng-Hsueh Lu,[‡] Yi-Feng Lai,[‡] Bao Lei,[†] Chuan-Pu Liu,[‡] and Yang Yang[†,*]

[†]Department of Materials Science and Engineering, University of California, Los Angeles, California 90095 and [‡]Department of Materials Science and Engineering, National Cheng Kung University, Tainan, Taiwan 701. [§]These authors contributed equally to this work.

ABSTRACT A multi-source/component spray coating process to fabricate the photoactive layers in polymer solar cells is demonstrated. Well-defined domains consisting of polymer:fullerene heterojunctions are constructed in ambient conditions using an alternating spray deposition method. This approach preserves the integrity of the layer morphology while forming an interpenetrating donor (D)/acceptor (A) network to facilitate charge transport. The formation of multi-component films without the prerequisite of a common solvent overcomes the limitations in conventional solution processes for polymer solar cells and enables us to process a wide spectrum of materials. Polymer solar cells based on poly(3-hexylthiophene):[6,6]-phenyl C_{61} butyric acid methyl ester spray-coated using this alternating deposition method deliver a power conversion efficiency of 2.8%, which is comparable to their blend solution counterparts. More importantly, this approach offers the versatility to independently select the optimal solvents for the donor and acceptor materials that will deliver well-ordered nanodomains. This method also allows the direct stacking of multiple photoactive polymers with controllable absorption in a tandem structure even without an interconnecting junction layer. The introduction of multiple photoactive materials through multisource/component spray coating offers structural flexibility and tenability of the photoresponse for future polymer solar cell applications.

KEYWORDS: spray coating · polymer solar cell · layer-by-layer deposition · interpenetrating network · photon recycling

Recent progress in polymer photovoltaics has allowed scientists to forge ahead on exploiting high-efficiency, low-cost solar cells for renewable energy applications.[1−4] In addition, the compatibility with flexible, large-area substrates contend polymer solar cells as attractive alternatives to their inorganic counterparts. The prospect of harnessing solar energy renders polymer solar cells a promising candidate for future solar cells.

Spin-coating is the dominant fabrication method in polymer solar cell research; however, it is neither high throughput nor scalable. To realize these requirements, a myriad of deposition methods such as inkjet printing,[5,6] screen printing,[7] doctor blading,[8,9] and spray coating[10,11] have all been adopted to pursue success in large-area coating. Amongst them, spray coating is capable of delivering large-area, uniform polymer thin films through a relatively simple process, offering ample processing possibilities of engineering the film structure. In this method, the film evolution is a reconstitution process whereby solution particles are atomized and driven by a carrier gas onto the substrate; therefore, the droplets and resulting domain sizes can be finely tuned *via* controlled atomization. Films with a broad range of concentration and composition can be delivered *via* the spray coating method, thus allowing for the straightforward processing of polymers with poor solubility,[11] as well as organic and inorganic materials with varying degrees of solubility/dispersity in the liquid phase. This opens up a whole new category of applications in materials chemistry.

The feasibility of utilizing commercially available airbrushes to fabricate both the electrodes[12,13] and photoactive layers[14−16] in polymer solar cells, as well as fully spray-coated organic photodiodes,[17] has been recently demonstrated. Here, we report a facile alternating deposition method, which establishes the foundations of the multi-component/source spray coating process. The key concept relies on the partial coverage of alternating donor (D)/ acceptor (A) layers to construct an interpenetrating network of nanodomains that mimics the nature of layer-by-layer (LbL) deposition. This alternating spray deposition enables the formation of multi-component films from independent sources regardless of their distinct material properties, which allows the application of a wide spectrum of material systems. To this end, we have demonstrated polymer solar cells by the alternating spray deposition approach to form a bicontinuous nanomorphology that facilitates exciton dissociation and charge trans-

*Address correspondence to yangy@ucla.edu.

Received for review December 3, 2009 and accepted July 26, 2010.

Published online August 6, 2010.
10.1021/nn901758p

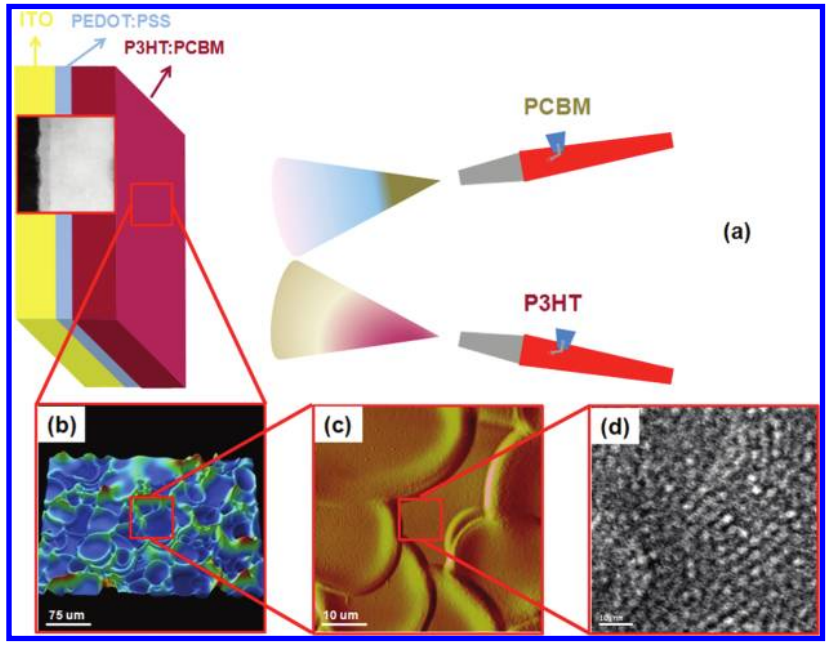

Figure 1. (a) Schematic of the alternating spray deposition apparatus. The device structure is shown with a TEM cross-sectional image, indicating the ITO/PEDOT:PSS/P3HT:PCBM layers starting from the left with well-defined interfaces. Zoom-in representative images taken from (b) optical profiler, (c) AFM, and (d) TEM of 150 °C annealed film from P3HT/PCBM alternating deposition.

portation. The advantages of spray coating from multiple sources were revealed by using solvents with selective solubilities to deliver well-ordered domains of both the donor and acceptors. This versatile approach can also be integrated with other material systems and processes to directly and precisely introduce functional building blocks resembling the ion implantation process. In fact, highly conformal spray coating of functional materials throughout porous substrates has recently been demonstrated.[18]

On the other hand, dissolution of layered deposition has hindered the wide inclusion of solution-processed photovoltaics. Through the alternating spray deposition approach, the underlying film can sustain the subsequent deposition and retain its structural integrity, thus a bilayer tandem structure with controllable absorption can be attained even without an interlayer for charge recombination.[19] By exploiting the advantages of the alternating spray deposition, a three-component interpenetrating network was also formed by partial coverage of the alternating polymer blends. The active layer comprises two polymer donor materials to form a multi-component pathway, where the photoresponse range can complement the solar spectrum, with the advantage of photon recycling.[20] Consequently, alternating spray deposition offers a straightforward way to achieve efficient light harvesting and an alternative approach to controlling the polymer film morphology.

RESULTS AND DISCUSSION

Chlorobenzene (CB) was chosen as the solvent for our spray coating process because solution droplets from CB exhibited intermediate viscosity for efficient and homogeneous deposition onto the substrate.[16] A polymer concentration of 5 mg/mL was chosen to provide a balance between the number of passes required and the amount of photoactive materials deposited. The active layers were spray-coated in ambient conditions for typically a few hundred passes until the desired absorbance (optical density) was reached. The details of the device fabrication and characterization are described in the Methods section.

Figure 1a shows the alternating spray deposition apparatus, with the P3HT and PCBM solutions as the multiple sources. For comparison, films spray-coated from the P3HT:PCBM blend solution were also fabricated. Optical microscopic images clearly indicate the droplet diameters ranging from 10 μm for a single droplet to several tens of micrometers for merged droplets. The thicknesses of the active layers are approximately 300 nm, with surface features extruding up to several hundreds of nanometers due to the "coffee-ring" effect.[21] Nevertheless, the typical rough topography (comparable to the film thickness) in spray-coated films only slightly deteriorates the device performance.[14]

The morphologies of the spray-coated films under different scales were characterized by several imaging tools. Figure 1b−d shows a series of film images obtained from the optical profiler, atomic force microscopy (AFM), and transmission electron microscopy (TEM), respectively, from the alternating spray deposition after annealing at 150 °C. The optical profiler image in Figure 1b displays droplet sizes of tens of micrometers. The ring-like deposits are due to the capillary flow such that continuous deposition partially dissolves the previous droplets and replenishes the liquid

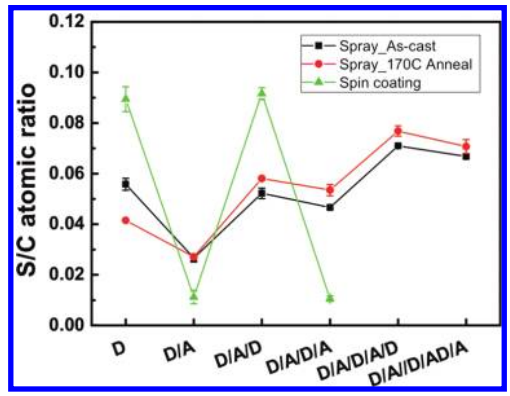

Figure 2. Sulfur to carbon (S/C) ratios calculated from the XPS analysis for as-cast and 170 °C annealed films from the first three cycles of P3HT/PCBM alternating spray deposition. D is for the donor P3HT, while A is for the acceptor PCBM. The S/C ratios from alternating spin coating of the P3HT and PCBM layers were also compared.

solution for resolidification at the pinned contact line.[21,22] The corresponding AFM phase image in Figure 1c also confirmed droplet features with flat plateaus surrounded by ridge-like features.[16] Note that thermal annealing does not induce any observable surface topography changes under the micrometer scale.

The inset of Figure 1a shows the TEM cross-sectional image, where the PEDOT:PSS (~30 nm) and the P3HT:PCBM layer (~300 nm) can be distinguished with well-defined interfaces. By defocusing the electron beam to 5 μm, the structural features are clearly observed in Figure 1d, where the bright and dark regions resemble the PCBM- and P3HT-rich domains, respectively.[23] The interconnected P3HT and PCBM domains appear broader and more continuous after thermal annealing. Using a correlation function calculation, stronger correlations also imply improved structural ordering for the annealed films (see Figure S1 in Supporting Information).[24]

One of the distinctive advantages of the alternating spray deposition is the resilience to subsequent coating that preserves the film structural integrity. A previous report estimated a drying time in the microsecond range for the spray-coated droplets, suggesting insufficient time for complete dissolution of the underlayer.[16] To provide an insight to the structural integrity, X-ray photoelectron spectroscopy (XPS) was carried out after the deposition of alternating P3HT/PCBM layers to evaluate the sulfur to carbon (S/C) ratio of the film surface. This clearly proves the periodic variation of the P3HT/PCBM ratio upon the alternating spray deposition.[25] The films examined were deposited by five passes of each material, similar to the device fabrication conditions. Each sample was examined at three different spots that were a few millimeters apart. Figure 2 shows that within the first three cycles of the alternating spray deposition, that is (P3HT/PCBM) × 3, zigzag variations of the S/C ratio were obtained for both as-cast and annealed films derived from the alternating

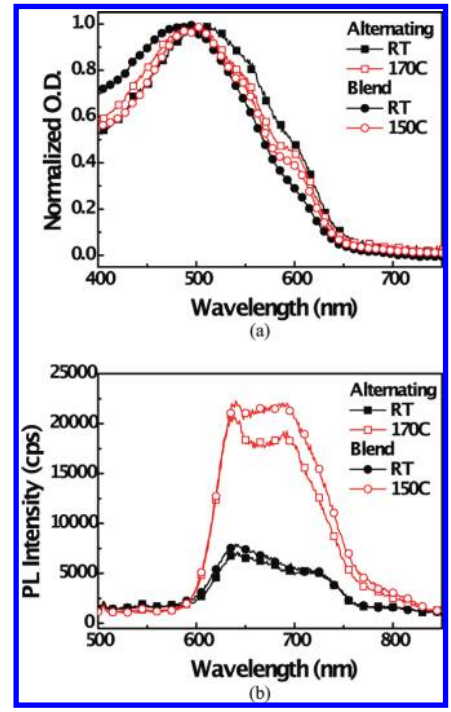

Figure 3. (a) Normalized absorption and (b) PL spectra for as-cast and annealed spray-coated films from P3HT/PCBM alternating deposition and P3HT:PCBM blend solution, respectively.

spray deposition. As expected from the partial coverage, the deposition of P3HT increases the S/C signal ratio, while a layer of PCBM reduces it. If the underlying layer was fully dissolved, strong sulfur signals should appear on the film surface after each deposition due to the lower surface energy of P3HT.[25,26] It is thus confirmed that the film structure of the underlayer was retained upon subsequent spray deposition.[27] On the contrary, the color changes from visual observation of the films from alternating spin coating of the P3HT and PCBM materials dissolved in CB readily suggest complete dissolution of the underlying layer. Furthermore, the dramatic variation in the S/C ratio also indicates almost complete dissolution of the underlying layer, with only trace amount of P3HT detected after spin coating of PCBM. The higher S/C ratio for annealed samples is due to the annealing process that drives P3HT to the surface to reduce the overall energy of the system.[25,26] Such evaluation of the S/C ratio offers a convenient implement to monitor the structural integrity for spray deposition.

To elucidate the optical properties, films spray-coated from two conditions, (1) directly from P3HT:PCBM blend solution and (2) alternatively from P3HT and PCBM solutions, were examined by UV−vis absorption and photoluminescence (PL) spectroscopy. The absorption spectra in Figure 3a were normalized to the maximum P3HT absorption for comparison. For as-cast films, the alternating film shows a significant red shift and vibronic feature at 610 nm, which is indicative of strong interplanar π−π stacking.[28−30] The enhanced

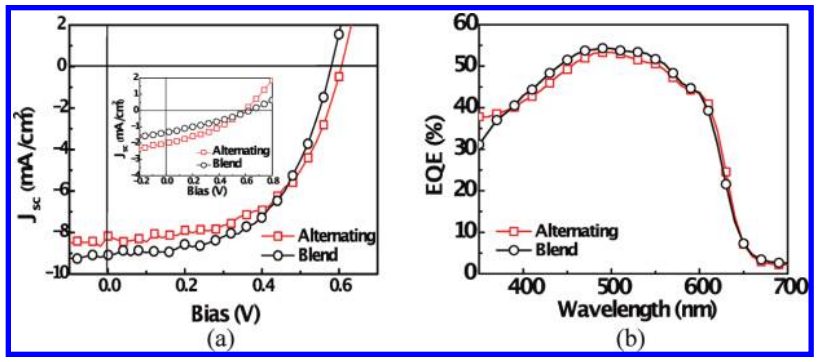

Figure 4. (a) Current density−voltage (*J*−*V*) curves of annealed spray-coated devices from P3HT/PCBM alternating deposition and P3HT:PCBM blend solution, respectively. The inset shows the *J*−*V* curves for as-cast devices, revealing the inherent advantage of the alternating spray deposition. (b) Corresponding EQE for the annealed spray-coated devices, with EQE maxima of 54%.

structural order can also be visualized by the purple color of as-cast films, whereas the films from the blend solution appear orange. Upon thermal annealing, both films exhibit the vibronic feature at 610 nm, analogous to the crystallinity of spin-coated films. The limited drying time of pristine polymer droplets still allows for self-organization of P3HT, unveiling the advantage of forming as-cast crystalline films from the alternating spray deposition. The absorption spectra also suggest that the subsequent deposition should at most slightly dissolve the underlayer; otherwise, the absorption spectra should be similar to the film from the blend solution. However, partial intermixing of the P3HT and PCBM domains is essential to provide the additional interfaces for exciton dissociation, which will be shown in the following.

In polymer photovoltaics, PL quenching is indicative of the exciton dissociation efficiency, which delivers a convincing fingerprint for the extent of phase separation.[30] Figure 3b compares the PL spectra of as-cast and annealed films with 480 nm excitation. The enhanced PL intensity after annealing implies reduced charge transfer efficiency due to domain growth and decreased nonradiative decay channels in the P3HT domains with increasing order.[30] The separation of the PL spectra into vibronic features upon annealing also designates ordered P3HT domains.[31,32] When matched to Figure 1, the alternating spray deposition spontaneously forms a three-dimensional D/A network with interpenetrating charge transport pathways. However, the network connection depends on the domain sizes, which can be precisely controlled by the partial coverage of each deposition rather than the phase separation concept demonstrated in traditional bulk heterojunctions. This method shares the common features with the controlled vacuum deposition of the D/A molecules to form the interpenetrating network throughout the bulk film.[33] Furthermore, the nanoscale morphology of spray-coated polymer films is independent of the vertical phase separation, making this a suitable technique to form the ideal vertical composition profile that facilitates charge collection, where the anode is P3HT-enriched and the cathode is PCBM-enriched.[25,26,34] Examples of controlled distribution and gradient junction polymer solar cells to realize an optimal vertical morphology by spray coating have been recently reported.[35,36]

The inherent advantage of the alternating spray deposition is revealed in the *J*−*V* characteristics shown in the inset of Figure 4a. As-cast films by the alternating deposition exhibit better device performance of 0.42% *versus* 0.27% PCE compared to its blend solution counterpart, with the detailed device characteristics listed in Table 1. The better performance is due to the spontaneously-formed crystalline D/A network for as-cast films from alternating spray deposition. Figure 4a shows the improved device performance upon annealing at optimal temperatures, with the alternating film exhibiting 2.8% PCE, which is comparable to the 2.9% efficiency obtained from the blend solution. The more continuous network contributed to the enhanced short-circuit current (J_{sc}), which is also evident from the reduction in series resistance (R_s). In comparison, P3HT:PCBM BHJ films spin-coated from a 2% blend solution (1:1 wt/wt ratio) in air and annealed at 110 °C for 10 min in the glovebox deliver a similar device performance of 3.2% PCE. Figure 4b shows the corresponding external quantum efficiency (EQE) spectra of the annealed devices, with EQE maxima of approximately 54%, and the evident photocurrent contribution from the vibronic shoulder for both devices. Due to the very short drying time of the films, conventional solvent annealing was not viable. However, by exposing the spray-coated films to saturated vapor of several sol-

TABLE 1. Photovoltaic Performance of As-Cast and Annealed Films Spray-Coated From P3HT/PCBM Alternating Deposition and P3HT:PCBM Blend Solution, Respectively

structure	anneal *T* [°C]	V_{oc} [V]	J_{sc} [mA/cm²]	PCE [%]	FF [%]	R_s [Ω cm²]
	rt	0.60	2.02	0.42	34.65	151.4
alternating	170	0.60	8.17	2.81	57.38	3.28
	RT	0.64	1.32	0.27	31.49	1998
blend	150	0.58	9.08	2.91	55.30	3.92

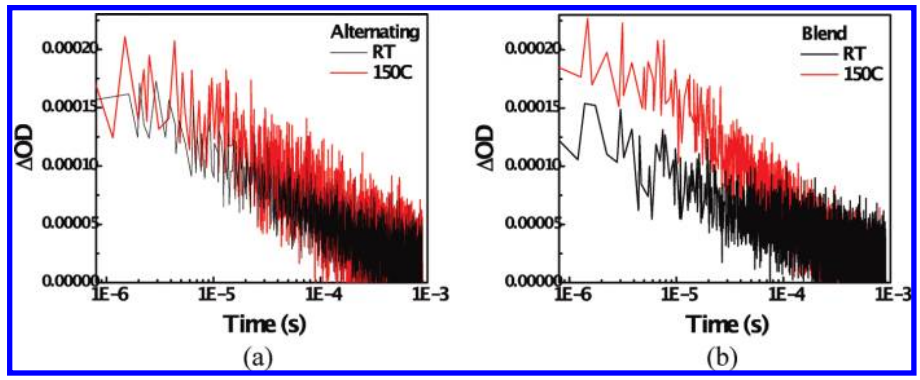

Figure 5. (a) Transient absorption spectroscopy results for as-cast and annealed spray-coated films from (a) P3HT/PCBM alternating deposition and (b) P3HT:PCBM blend solution, using a 510 nm dye laser pumped by a nitrogen laser as the excitation source.

vents, we observed a similar effect on improving the crystallinity and device performance (J_{sc} and FF) but less pronounced than the thermal annealing treatment.[30,37]

To confirm the correlation between P3HT crystallinity and photovoltaic performance, transient absorption spectroscopy (TAS) was used to study the charge carrier dynamics according to the change of optical density (ΔOD) signal amplitude (see Supporting Information S2 for setup details). It has been proposed that free carrier generation in the BHJs is correlated to the free energy of charge separation, that is, ΔG_{CS}^{eff}, the difference between exciton energy and polaron pair energy.[38,39] Furthermore, annealing can shift the highest occupied molecular orbital (HOMO) level of P3HT due to improved crystallinity, while the band gap remains unchanged. Figure 5a,b compares the photogeneration efficiency of the spray-coated films, showing more efficient charge generation for the alternating spray deposition in the as-cast film, which can be attributed to the larger ΔG_{CS}^{eff} due to higher $\pi-\pi$ stacking of P3HT chains, as evidenced from the UV−vis absorption spectra in Figure 3a. The negligible influence of thermal annealing on the photogeneration efficiency suggests that the increased photocurrent is due to improved charge transport pathways. This is consistent with the unchanged V_{oc} of the alternating film upon annealing (Figure 4a), implying that thermal annealing does not contribute to an observable HOMO shift of P3HT in this case. The improved demixing of the P3HT and PCBM domains may be responsible for the decreased carrier recombination and thus increased J_{sc}; however, the detailed mechanism is still under study. On the contrary, Figure 5b shows a significant increase in the photogeneration yield for the film prepared from the blend solution after thermal annealing due to enhanced crystallinity and thus charge generation, which agrees with previous reports.[39] Meanwhile, reduction of the V_{oc} of the photovoltaic cell from the blend solution from 0.64 to 0.58 V after thermal annealing strongly suggests a significant change in the HOMO level of P3HT. The transient absorption results hence validate that the alternating spray deposition provides an alternative approach to controlling the polymer morphology, along with the annealing processes.

The versatile alternating spray deposition offers the freedom to deposit the donor and acceptor materials independently to form a bicontinuous network of interpenetrating D/A domains. Employing this advantage, alternating spray deposition from solvents with selective solubility can deliver photovoltaic devices regardless of the solvent compatibility. An example of this is a device consisting of alternating solutions of P3HT in chloroform and PCBM in *p*-xylene, which was proposed to exhibit strong solvent−solute interaction.[40] Figure 6a compares the absorption spectra of the films as-cast and annealed at 110 and 170 °C. Note that the promi-

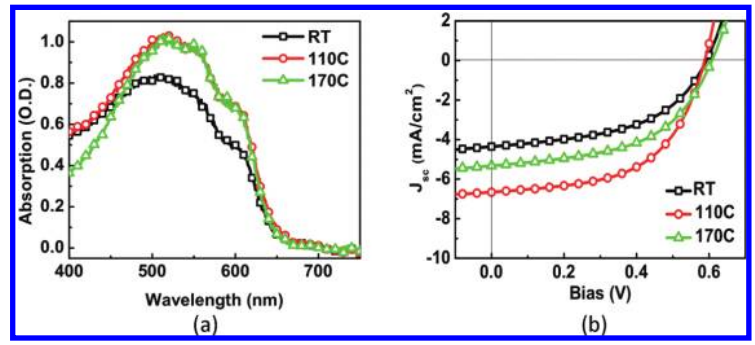

Figure 6. (a) UV−vis absorption spectra and (b) *J*−*V* characteristics of the P3HT/PCBM films from alternating deposition of different solvents, as-cast and annealed at 110 and 170 °C. The solvents carrying P3HT and PCBM were chloroform and *p*-xylene, respectively.

TABLE 2. Photovoltaic Performance of a Spray-Coated PSBTBT:PCBM Film, Bilayer Films Spray-Coated with Different Sequences of Alternating P3HT:PCBM and PSBTBT:PCBM Blend Solutions, and a Three-Component BHJ Cell Consisting of PSBTBT:PCBM:P3HT[a]

structure	V_{oc} [V]	J_{sc} [mA/cm^2]	PCE [%]	FF [%]	R_s [Ω cm^2]
PSBTBT:PCBM reference	0.64	10.11	2.66	41.10	4.14
P3HT:PCBM(20)/PSBTBT:PCBM(170)	0.66	7.71	2.23	43.75	4.51
PSBTBT:PCBM(90)/P3HT:PCBM(110)	0.62	7.87	2.28	46.70	4.15
PSBTBT:PCBM:P3HT	0.60	6.88	1.88	45.56	3.59

[a]The number in the parentheses indicates the number of coatings.

nent shoulder at 610 nm indicates the existence of ordered P3HT chains even for as-cast films. The $J-V$ characteristics of Figure 6b show that the as-cast device achieved a 1.3% PCE, with a V_{oc} of 0.59 V, J_{sc} of 4.35 mA/cm^2, FF of 50.4%, and R_s of 4.24 Ω cm^2. This encouraging result strongly substantiates the intrinsic advantage of the multi-source spray coating to spontaneously form an interpenetrating D/A network by selecting the appropriate solvent for each component. The device performance improves to 2.17% after annealing at 110 °C, with a V_{oc} of 0.59 V, J_{sc} of 6.66 mA/cm^2, FF of 55.4%, and R_s of 1.75 Ω cm^2. The device performance slightly deteriorates upon higher temperature annealing due to the larger degree of phase separation, which increases the R_s. This approach thus offers the versatility to select the optimal solvent for the donor and acceptor materials and overcomes the prerequisite of a common solvent in polymer blend solutions. Accordingly, the utilization of material systems with a lower degree of phase separation to deliver ordered D/A networks, which is inhibited in the spin-coating processes, substantially broadens the choice of materials for photovoltaic application. Further applications of this deposition technique include, but are not limited to, incorporation of dopants and functional layers in light-emitting devices[41,42] and light-scattering materials for solar cells.[43]

The solvent mixture effects were also investigated in the alternating spray deposition.[44] Systematical study of solvent systems have been demonstrated in the spin-coating process to assist the formation of ordered structure without any further treatment.[44−46] When 2 vol % 1,8-octanedithiol (OT) was incorporated into the P3HT solution (in CB) for the alternating spray deposition, the enhanced ordering of the P3HT domains improved the PCE from 0.41 to 1.55% without any annealing treatment or device optimization (see Supporting Information S3). The decisive role of solvent mixtures in spray coating process is yet to be clarified, but the beneficial improvement in structural ordering can already be recognized.

The underlying film structure is robust enough to sustain the subsequently spray-coated top layer, thus a double active layer tandem structure with controllable absorption range and intensity can be achieved by the alternating spray deposition even without an interlayer. Interlayer-free multi-junction polymer solar cells are realized here with a double active layer consisting of two polymer blend systems: P3HT and poly[(4,42-bis(2-ethylhexyl)dithieno[3,2-*b*:22,32-*d*]silole)-2,6-diyl-*alt*-(2,1,3-benzothiadiazole)-4,7-diyl] (PSBTBT) blended with PCBM.[47,48] PSBTBT was chosen due to its distinct absorption in the near-IR range and similar HOMO level with P3HT. The absorption intensity of each active layer can be easily tuned by the thickness and sequence of individual layer depositions. Table 2 lists the detailed performances for the P3HT:PCBM/PSBTBT:PCBM bilayer devices, with similar performances of ∼2.3% PCE based on distinct EQE spectra validated from the EQE spectra in Figure 7a. The EQE spectra of a spray-coated reference PSBTBT:PCBM film (3.2% PCE) was also shown for comparison, exhibiting a 35% EQE maxima at 700 nm. Major limitation of the PCE is the low EQE maxima (<40%), which should substantially increase upon optimizing the relative thickness of the absorption layers. Another PCE limitation is the low FF (<50%), which is probably due to the HOMO level mismatch (∼0.1 eV) between P3HT and PSBTBT that hampers the hole transport.

In the alternating spray deposition, the layers can also be varied for an alternative multi-component film structure. We observed enhanced photoresponse from proof-of-concept device with 1.88% PCE, in which P3HT:PCBM and PSBTBT:PCBM are the multiple sources, forming interconnected networks of P3HT/PCBM/PSBTBT domains. This heterojunction distinguishes itself from conventional BHJ films derived from a single solution containing multiple components, where the third component usually impedes the phase separation process, and introduces either energy barriers or carrier traps that are detrimental for charge transportation.[49] This method holds tremendous potential in realizing photon recycling *via* either energy transfer or optical reabsorption.[20] In the P3HT/PCBM/PSBTBT system, excess excitons generated in P3HT domains might not be able to reach the donor−acceptor interface for charge dissociation.[50] With the presence of the lower band gap PSBTBT in the vicinity, these excitons may be harvested again *via* reabsorption or energy transfer to contribute to the photocurrent. In the P3HT:PCBM and PSBTBT:PCBM (5:1 ratio) alternating structure, the absorption profile in Figure 7b confirms the recovery of

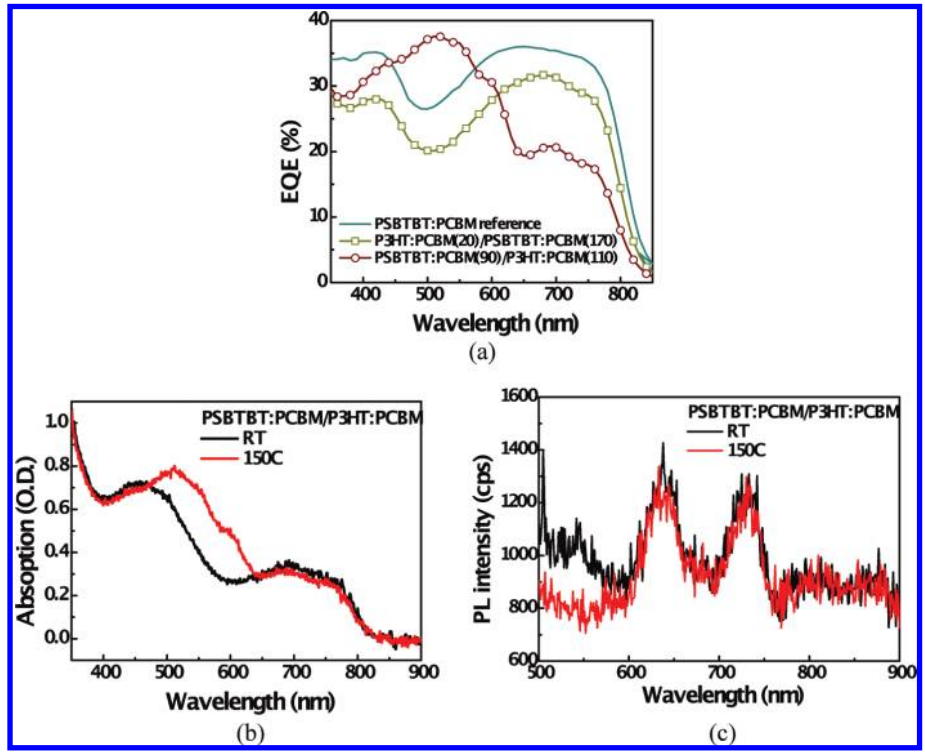

Figure 7. (a) EQE spectra of a reference PSBTBT:PCBM cell and P3HT:PCBM and PSBTBT:PCBM bilayer films of different relative thickness and sequences. The number in the parentheses indicates the number of deposition passes. (b) UV−vis absorption and (c) PL spectra for the three-component heterojunction films spray-coated from alternating P3HT:PCBM/PSBTBT: PCBM solutions before and after annealing at 150 °C.

P3HT crystallinity upon annealing from the slight intermixing of P3HT and PSBTBT. In contrast to the P3HT:PCBM films, Figure 7c shows the PL emission intensity on the same order upon annealing, suggesting that the PL from P3HT is either quenched or reabsorbed by PSBTBT. The three-component P3HT/PCBM/PSBTBT heterojunction device delivers a PCE of 1.88%, with the detailed device characteristics listed in Table 2. The importance of this photon-recycling design can be benefited by collecting the excess excitons that are not quenched due to poor crystallinity in certain polymer solar cell systems.

CONCLUSIONS

In conclusion, three-dimensional interpenetrating networks of polymer donors and fullerene acceptors, which are essential for high-performance polymer solar cells, have been achieved *via* a multisource/component alternating spray deposition process mimicking the layer-by-layer (LbL) deposition. Our investigation into the film morphology suggests that this approach offers precise control over the D/A domain network, providing an alternative way to manipulate the domain formation and phase separation in polymer blend films without using conventional annealing processes. Utilizing this deposition method, the film integrity can be preserved upon subsequent depositions and allows the demonstration of heterojunctions with active layers composed of bilayer structures or three-component systems. This approach also features a series of advantages over conventional solution processes, to name a few, enabling deposition of materials from lower concentrations and distinct solutions, which significantly broaden the selection of material systems. Therefore, this versatile deposition technique provides a powerful tool to realize various design and functionality of organic electronic devices and forecasts competitive polymer photovoltaics for renewable energy applications.

METHODS

Device Fabrication. The spray coating solutions were 5 mg/mL P3HT (or PCBM) in chlorobenzene (CB) for the alternating deposition and 5 mg/mL P3HT:PCBM (1:1 wt ratio) for the blend solution. For the selective solvents, the concentration of P3HT and PCBM was 5 mg/mL in chloroform and *p*-xylene, respectively. The device configuration is ITO/PEDOT:PSS/active layer/Ca/Al. The ITO substrates were precleaned with ultrasonic treatment in detergent, deionized water, acetone, and isopropyl alcohol sequentially and treated with UV-ozone for 15 min prior to the film deposition. The PEDOT:PSS layer (Baytron P VP AI 4083) was spin-coated at 4000 rpm for 40 s and subsequently annealed at 150 °C for 10 min. The active layers were spray-coated in ambient conditions for typically a few hundred passes, until the desired absorbance (optical density) was reached. To simplify the experi-

mental conditions, the film thickness was controlled by adjusting the nozzle size and the number of passes. Nitrogen with a pressure of 15 psi was used as the carrier gas with the distance between the nozzle tip and the substrate held at 12 cm.

After film deposition, the polymer films were transferred to a nitrogen-filled glovebox and annealed at optimal temperatures for 10 min. The Ca/Al electrodes were thermally evaporated at 2×10^{-6} Torr, with thicknesses of 25 and 100 nm, respectively.

Device Characterization. The devices were tested in a nitrogen-filled glovebox under simulated AM 1.5 G irradiation (100 mW/cm^2) using an Oriel 96000 150 W solar simulator (Newport Corporation), with a Schott visible-color glass-filtered (KG5 color filtered) Si diode (Hamamatsu S1133) calibrated to National Renewable Energy Lab.[51] The EQE spectra of the encapsulated devices were measured using a lock-in amplifier (SR830, Stanford Research Systems) under short-circuit conditions when the devices were illuminated by monochromatic light from a xenon lamp passing through a monochromator (SpectraPro-2150i, Acton Research Corporation).

Analysis. The XPS analysis was carried out in an Omicron Nanotechnology system with a base pressure of 2×10^{-10} Torr with Al Ka radiation (1486.6 eV) as the excitation source. The absorption spectra were obtained from a Varian Cary 50 UV−visible spectrometer. The PL spectra were taken from FluoroLog-3 by Horiba Jobin Yvon, with 480 nm excitation. A Veeco Wyko NT9300 optical profiler was used for the three-dimensional surface mapping. Veeco Dimension 5000 scanning probe microscope was used for the atomic force microscopic (AFM) imaging. The cross-sectional samples were prepared using a dual-beam focused ion beam (DB-FIB, FEI Nova-200 Nano-Lab Compatible) system. The high-resolution transmission electron microscopy (HRTEM) images were taken with JEOL-2100F at 200 keV in a through-focus series.

Acknowledgment. The authors acknowledge Dr. Y. Wu for originating the idea, Dr. J.-H. Li and R. Green for initiating the experiment, Dr. S. Jonas and Dr. J. Reed for their expertise with instrumentation, Dr. V. Tung for helpful discussions, and the UCLA CNSI Pico Lab for the imaging. Financial support from Office of Naval Research (ONR) is appreciated. L.-M.C. also acknowledges financial support from NSF IGERT: Materials Creation Training Program (MCTP) (DGE-0114443) and California NanoSystems Institute (CNSI).

Supporting Information Available: More details regarding the TEM images, correlation function calculation, device characteristics of alternating spray deposition with OT addition, as well as transient absorption measurement setup are presented. This material is available free of charge *via* the Internet at http://pubs.acs.org.

REFERENCES AND NOTES

1. Li, G.; Shrotriya, V.; Huang, J.; Yao, Y.; Moriarty, T.; Emery, K.; Yang, Y. High-Efficiency Solution Processable Polymer Photovoltaic Cells by Self-Organization of Polymer Blends. *Nat. Mater.* **2005**, *4*, 864–868.
2. Ma, W.; Yang, C.; Gong, X.; Lee, K.; Heeger, A. J. Thermally Stable, Efficient Polymer Solar Cells with Nanoscale Control of the Interpenetrating Network Morphology. *Adv. Funct. Mater.* **2005**, *15*, 1617–1622.
3. Park, S. H.; Roy, A.; Beaupre, S.; Cho, S.; Coates, N.; Moon, J. S.; Moses, D.; Leclerc, M.; Lee, K.; Heeger, A. J. Bulk Heterojunction Solar Cells with Internal Quantum Efficiency Approaching 100%. *Nat. Photonics* **2009**, *3*, 297–302.
4. Chen, H.-Y.; Hou, J. H.; Zhang, S. Q.; Liang, Y. Y.; Yang, G. W.; Yang, Y.; Yu, L. P.; Wu, Y.; Li, G. Polymer Solar Cells with Enhanced Open-Circuit Voltage and Efficiency. *Nat. Photonics* **2009**, *3*, 649–653.
5. Chang, S.-C.; Liu, J.; Bharathan, J.; Yang, Y.; Onohara, J.; Kido, J. Multicolor Organic Light-Emitting Diodes Processed by Hybrid Inkjet Printing. *Adv. Mater.* **1999**, *11*, 734–737.
6. Marin, V.; Holder, E.; Wienk, M. M.; Tekin, E.; Kozodaev, D.; Schubert, U. Ink-Jet Printing of Electron Donor/Acceptor Blends: Towards Bulk Heterojunction Solar Cells. *Macromol. Rapid Commun.* **2005**, *26*, 319–324.
7. Shaheen, S. E.; Radspinner, R.; Peyhambarian, N.; Jabbour, G. E. Fabrication of Bulk Heterojunction Plastic Solar Cells by Screen Printing. *Appl. Phys. Lett.* **2001**, *79*, 2996–2998.
8. Schilinsky, P.; Waldauf, C.; Brabec, C. J. Performance Analysis of Printed Bulk Heterojunction Solar Cells. *Adv. Funct. Mater.* **2006**, *16*, 1669–1672.
9. Chang, Y.-H.; Tseng, S.-R.; Chen, C.-Y.; Meng, H.-F.; Chen, E.-C.; Horng, S.-F.; Hsu, C.-S. Polymer Solar Cell by Blade Coating. *Org. Electron.* **2009**, *10*, 741–746.
10. Ishikawa, T.; Nakamura, M.; Fujita, K.; Tsutsui, T. Preparation of Organic Bulk Heterojunction Photovoltaic Cells by Evaporative Spray Deposition from Ultradilute Solution. *Appl. Phys. Lett.* **2004**, *84*, 2424–2426.
11. Green, R.; Morfa, A.; Ferguson, A. J.; Kopidakis, N.; Rumbles, G.; Shaheen, S. E. Performance of Bulk Heterojunction Photovoltaic Devices Prepared by Airbrush Spray Deposition. *Appl. Phys. Lett.* **2008**, *92*, 033301.
12. Lim, Y.-F.; Lee, S.; Herman, D. J.; Lloyd, M. T.; Anthony, J. E.; Malliaras, G. G. Spray-Deposited Poly(3,4-ethylenedioxythiophene):Poly(styrenesulfonate) Top Electrode for Organic Solar Cells. *Appl. Phys. Lett.* **2008**, *93*, 193301.
13. Hau, S. K.; Yip, H.-L.; Leong, K; Jen, A. K.-Y. Spraycoating of Silver Nanoparticle Electrodes for Inverted Polymer Solar Cells. *Org. Electron.* **2009**, *10*, 719–723.
14. Steirer, K. X.; Reese, M. O.; Rupert, B. L.; Kopidakis, N.; Olson, D. C.; Collins, R. T.; Ginley, D. S. Ultrasonic Spray Deposition for Production of Organic Solar Cells. *Sol. Energy Mater. Sol. Cells* **2009**, *93*, 447–453.
15. Hoth, C. N.; Steim, R.; Schilinsky, P.; Choulis, S. A.; Tedde, S. F.; Hayden, O.; Brabec, C. J. Topographical and Morphological Aspects of Spray Coated Organic Photovoltaics. *Org. Electron.* **2009**, *10*, 587–593.
16. Girotto, C.; Rand, B. P.; Genoe, J.; Heremans, P. Exploring Spray Coating as a Deposition Technique for the Fabrication of Solution-Processed Solar Cells. *Sol. Energy Mater. Sol. Cells* **2009**, *93*, 454–458.
17. Tedde, S. F.; Kern, J.; Sterzl, T.; Fürst, J.; Lugli, P.; Hayden, O. Fully Spray Coated Organic Photodiodes. *Nano Lett.* **2009**, *9*, 980–983.
18. Krogman, K. C.; Lowery, J. L.; Zacharia, N. S.; Rutledge, G. C.; Hammond, P. T. Spraying Asymmetry into Functional Membranes Layer-by-Layer. *Nat. Mater.* **2009**, *8*, 512–518.
19. Ameri, T.; Dennler, G.; Lungenschmied, C.; Brabec, C. J. Organic Tandem Solar Cells: A Review. *Energy Environ. Sci.* **2009**, *2*, 347–363.
20. Nelson, J. *the Physics of Solar Cells*; Imperial College Press: London, UK, 2003; Chapter 9.
21. Deegan, D.; Bakajin, O.; Dupont, T. F.; Huber, G.; Nagel, S. R.; Witten, T. A. Capillary Flow as the Cause of Ring Stains from Dried Liquid Drops. *Nature* **1997**, *389*, 827–829.
22. Kawase, T.; Sirringhaus, H.; Friend, R. H.; Shimoda, T. Inkjet Printed *via* Hole Interconnections and Resistors for All-Polymer Transistor Circuits. *Adv. Mater.* **2001**, *13*, 1601–1605.
23. Moon, J. S.; Lee, J. K.; Cho, S.; Byun, J.; Heeger, A. J. Columnlike" Structure of the Cross-Sectional Morphology of Bulk Heterojunction Materials. *Nano Lett.* **2008**, *9*, 230–235.
24. Lei, B.; Yao, Y.; Kumar, A.; Yang, Y.; Ozolins, V. Quantifying the Relation between the Morphology and Performance of Polymer Solar Cells Using Monte Carlo Simulations. *J. Appl. Phys.* **2008**, *104*, 024504.
25. Xu, Z.; Chen, L.-M.; Yang, G. W.; Huang, C.-H.; Hou, J. H.; Wu, Y.; Li, G.; Hsu, C.-S.; Yang, Y. Vertical Phase Separation in Poly(3-hexylthiophene): Fullerene Derivative Blends and Its Advantage for Inverted Structure Solar Cells. *Adv. Funct. Mater.* **2009**, *19*, 1227–1234.
26. Campoy-Quiles, M.; Ferenczi, T.; Agostinelli, T.; Etchegoin, P. G.; Kim, Y.; Anthopoulos, T. D.; Stavrinou, P. N.; Bradley,

D. D. C.; Nelson, J. Morphology Evolution *via* Self-Organization and Lateral and Vertical Diffusion in Polymer: Fullerene Solar Cell Blends. *Nat. Mater.* **2008**, *7*, 158–164.
27. Vak, D.; Kim, S.-S.; Jo, J.; Oh, S.-H.; Na, S.-I.; Kim, J.; Kim, D.-Y. Fabrication of Organic Bulk Heterojunction Solar Cells by a Spray Deposition Method for Low-Cost Power Generation. *Appl. Phys. Lett.* **2007**, *91*, 081102.
28. Chen, T.-A.; Wu, X.; Rieke, R. D. Regiocontrolled Synthesis of Poly(3-alkylthiophenes) Mediated by Rieke Zinc: Their Characterization and Solid-State Properties. *J. Am. Chem. Soc.* **1995**, *117*, 233–244.
29. Sirringhaus, H.; Brown, P. J.; Friend, R. H.; Nielsen, M. M.; Bechgaard, K.; Langeveld-Voss, B. M. W.; Spiering, A. J. H.; Janssen, R. A. J.; Meijer, E. W.; Herwig, P.; de Leeuw, D. M. Two-Dimensional Charge Transport in Self-Organized, High-Mobility Conjugated Polymers. *Nature* **1999**, *401*, 685–688.
30. Li, G.; Yao, Y.; Yang, H.; Shrotriya, V.; Yang, G. W.; Yang, Y. Solvent Annealing Effect in Polymer Solar Cells Based on Poly(3-hexylthiophene) and Methanofullerenes. *Adv. Funct. Mater.* **2007**, *17*, 1636–1644.
31. Korovyanko, O. J.; Österbacka, R.; Jiang, X. M.; Vardeny, Z. V.; Janssen, R. A. J. Photoexcitation Dynamics in Regioregular and Regiorandom Polythiophene Films. *Phys. Rev. B* **2001**, *64*, 235122.
32. Pope, M.; Swenberg, C. E. *Electronic Processes in Organic Crystals and Polymers*, 2nd ed.; Oxford University Press, Inc: New York, 1998.
33. Hiramoto, M.; Fujiwara, H.; Yokoyama, M. Three-Layered Organic Solar Cell with a Photoactive Interlayer of Codeposited Pigments. *Appl. Phys. Lett.* **1991**, *58*, 1062–1064.
34. Chen, L.-M.; Hong, Z.; Li, G.; Yang, Y. Recent Progress in Polymer Solar Cells: Manipulation of Polymer:Fullerene Morphology and the Formation of Efficient Inverted Polymer Solar Cells. *Adv. Mater.* **2009**, *21*, 1434–1449.
35. Mo, X. L.; Mizokuro, T.; Kobayashi, A.; Chen, G.; Tanigaki, N.; Hiraga, T. Fabrication of Polymer Thin Films with In-Depth Dye-Dispersed Structures by the Vacuum Spray Method. *Thin Solid Films* **2008**, *516*, 1663–1668.
36. Shakutsui, M.; Iwamoto, T.; Maeda, R.; Tsutsui, T.; Fujita, K. Fabrication of Bulk Heterojunction Photovoltaic Cells with Controlled Distribution of p−n Components by Evaporative Spray Deposition Using Ultradilute Solution. *Proc. SPIE* **2008**, *7052*, 705215-1.
37. Zhao, Y.; Xie, Z.; Qu, Y.; Geng, Y. H.; Wang, L. X. Solvent-Vapor Treatment Induced Performance Enhancement of Poly(3-hexylthiophene):Methanofullerene Bulk-Heterojunction Photovoltaic Cells. *Appl. Phys. Lett.* **2007**, *90*, 043504.
38. Clarke, T. M.; Ballantyne, A. M.; Nelson, J.; Bradley, D. D. C.; Durrant, J. R. Free Energy Control of Charge Photogeneration in Polythiophene/Fullerene Solar Cells: The Influence of Thermal Annealing on P3HT/PCBM Blends. *Adv. Funct. Mater.* **2008**, *18*, 4029–4035.
39. Okhita, H.; Cook, S.; Astuti, Y.; Duffy, W.; Tierney, S.; Zhang, W.; Heeney, M.; McCulloch, I.; Nelson, J.; Bradley, D. D. C.; Durrant, J. R. Charge Carrier Formation in Polythiophene/Fullerene Blend Films Studied by Transient Absorption Spectroscopy. *J. Am. Chem. Soc.* **2008**, *130*, 3030–3042.
40. Chen, C.-C. Study of Cosolvent Techniques in Manufacturing Large Area Flexible Organic Photovoltaic Modules. MS. Dissertation, National Chiao Tung University, Hsinchu, Taiwan, April, 2009.
41. Huang, J.; Hou, W.-J.; Li, J.-H.; Li, G.; Yang, Y. Improving the Power Efficiency of White Light-Emitting Diode by Doping Electron Transport Material. *Appl. Phys. Lett.* **2006**, *89*, 133509.
42. Huang, J.; Li, G.; Wu, E.; Xu, Q.; Yang, Y. Achieving High-Efficiency Polymer White-Light-Emitting Devices. *Adv. Mater.* **2006**, *18*, 114–117.
43. Zhu, K.; Neale, N. R.; Miedaner, A.; Frank, A. J. Enhanced Charge-Collection Efficiencies and Light Scattering in Dye-Sensitized Solar Cells Using Oriented TiO_2 Nanotubes Arrays. *Nano Lett.* **2007**, *7*, 69–74.
44. Yan, Y.; Hou, J. H.; Xu, Z.; Li, G.; Yang, Y. Effects of Solvent Mixtures on the Nanoscale Phase Separation in Polymer Solar Cells. *Adv. Funct. Mater.* **2008**, *18*, 1783–1789.
45. Peet, J.; Kim, J. Y.; Coates, N. E.; Ma, W. L.; Moses, D.; Heeger, A. J.; Bazan, G. C. Efficiency Enhancement in Low-Bandgap Polymer Solar Cells by Processing with Alkane Dithiols. *Nat. Mater.* **2007**, *6*, 497–500.
46. Chen, H.-Y.; Yang, H. C.; Yang, G. W.; Sista, S.; Zadoyan, R.; Li, G.; Yang, Y. Fast-Grown Interpenetrating Network in Poly(3-hexylthiophene):Methanofullerenes Solar Cells Processed with Additive. *J. Phys. Chem. C* **2009**, *113*, 7946–7953.
47. Hou, J. H.; Chen, H.-Y.; Zhang, S.; Li, G.; Yang, Y. Synthesis, Characterization, and Photovoltaic Properties of a Low Band Gap Polymer Based on Silole-Containing Polythiophenes and 2,1,3-Benzothiadiazole. *J. Am. Chem. Soc.* **2008**, *130*, 16144–16145.
48. Sista, S.; Park, M.-H.; Hong, Z.; Wu, Y.; Hou, J.; Kwan, W. L.; Li, G.; Yang, Y. Highly Efficient Tandem Polymer Photovoltaic Cells. *Adv. Mater.* **2010**, *22*, 380–383.
49. McNeill, C. R.; Halls, J. J. M.; Wilson, R.; Whiting, G. L.; Berkebile, S.; Ramsey, M. G.; Friend, R. H.; Greenham, N. C. Efficient Polythiophene/Polyfluorene Copolymer Bulk Heterojunction Photovoltaic Devices: Device Physics and Annealing Effects. *Adv. Funct. Mater.* **2008**, *18*, 2309–2321.
50. Li, G.; Shrotriya, V.; Yao, Y.; Huang, J.; Yang, Y. Manipulating Regioregular Poly(3-hexylthiophene):[6,6]-Phenyl-C_{61}-Butyric Acid Methyl Ester Blends—Route towards High Efficiency Polymer Solar Cells. *J. Mater. Chem.* **2007**, *17*, 3126–3140.
51. Shrotriya, V.; Li, G.; Yao, Y.; Moriarty, T.; Emery, K.; Yang, Y. Accurate Measurement and Characterization of Organic Solar Cells. *Adv. Funct. Mater.* **2006**, *16*, 2016–2023.